第36卷第9期 无 机 化 学 学 报 Vol.36 No.9
2020年9月 CHINESE JOURNAL OF INORGANIC CHEMISTRY 1763-1773

基于二甲基苯并联咪唑的钌(Ⅱ)多吡啶配合物的合成、光谱和电化学性质

曹曼丽[1,2] 尚美洁[3] 刘文婷[1,2] 尹 伟[1,2] 姚苏洋*[,1,2] 叶保辉*[,3]
([1]广东第二师范学院化学系,广州 510303)
([2]广东省普通高校先进材料与节能减排工程技术开发中心,广州 510303)
([3]中山大学化学学院,广州 510275)

摘要: 合成了一组钌多吡啶化合物$[Ru(bpy)_2(DMBbimH_x)]^{y+}$ (bpy=2,2′-联吡啶,$DMBbimH_2$=7,7′-二甲基-2,2′-苯并联咪唑,**1-A**:x=2;y=2;**1-B**:x=1,y=1;**1-C**:x=0,y=0)并测试了它们的核磁氢谱、紫外吸收和电化学性质。随着$DMBbimH_x$配体逐个脱去质子,配合物的光谱和电化学性质发生明显的变化。有趣的是,脱去一个质子的配合物**1-B**在不同极性的二氯甲烷和乙腈中的电化学性质呈现明显的差异:在二氯甲烷中,单核的**1-B**却能发生两步氧化,这是因为在弱极性的溶剂中,$[Ru(bpy)_2(DMBbimH)]^+$阳离子通过氢键结合形成二聚体,$[Ru(bpy)_2(DMBbimH)]^+$阳离子间存在质子耦合电子传递现象。在**1-B**的二氯甲烷溶液中得到了化合物$[Ru(bpy)_2(DMBbimH)]PF_6\cdot 2CH_2Cl_2$ (**2**)的单晶。晶体结构分析表明$[Ru(bpy)_2(DMBbimH)]^+$阳离子确实通过氢键结合形成二聚体,这与电化学测试的结果一致。而在极性较大的乙腈中,氢键二聚体不能稳定存在,在循环伏安曲线上只有一个峰存在。

关键词: 钌多吡啶配合物; 苯并联咪唑; 电化学; 质子耦合电子传递(PCET); 晶体结构
中图分类号: O614.82+1 **文献标识码:** A **文章编号:** 1001-4861(2020)09-1773-11
DOI: 10.11862/CJIC.2020.204

Synthesis, Spectroscopic and Electrochemical Properties of Ruthenium(Ⅱ) Polypyridyl Complexes with Dimethyl-bibenzimidazolate Ligands

CAO Man-Li[1,2] SHANG Mei-Jie[3] LIU Wen-Ting[1,2] YIN Wei[1,2] YAO Su-Yang*[,1,2] YE Bao-Hui*[,3]
([1]*Department of Chemistry, Guangdong University of Education, Guangzhou* 510303, *China*)
([2]*Engineering Technology Development Center of Advanced Materials & Energy Saving and Emission Reduction in Guangdong Colleges and Universities, Guangzhou* 510303, *China*)
([3]*MOE Key Laboratory of Bioinorganic and Synthetic Chemistry, School of Chemistry, Sun Yat-sen University, Guangzhou* 510275, *China*)

Abstract: A family of ruthenium(Ⅱ) polypyridyl complexes, namely $[Ru(bpy)_2(DMBbimH_x)]^{y+}$ (bpy=2,2′-bipyridine, $DMBbimH_2$=7,7′-dimethyl-2,2′-bibenzimidazole, **1-A**: x=2, y=2; **1-B**: x=1, y=1; **1-C**: x=0, y=0), were synthesized and determined by ^{1}H NMR, UV-Vis absorption and electrochemical measurements. With the deprotonation of N-H in $DMBbimH_x$ ligands, the spectroscopic and electrochemical properties of complexes showed evident differences. Interestingly, the electrochemical properties of mono-deprotonated **1-B** behaved very differently in dichloromethane and acetonitrile, which is due to different polarities of the solvents. In dichloromethane, mononuclear complex **1-B** underwent a two-step oxidation. This is because $[Ru(bpy)_2(DMBbimH)]^+$ cations are bonded by hydrogen bonds to form dimers in weakly polar solvent, and proton-coupled electron transfer (PCET) exists between the $[Ru(bpy)_2(DMBbimH)]^+$ cations. Single crystals of $[Ru(bpy)_2(DMBbimH)]PF_6\cdot 2CH_2Cl_2$ (**2**) were obtained from the solution of

收稿日期:2020-02-03。收修改稿日期:2020-05-23。
国家自然科学基金(No.21001031)、2019年广东省教育厅“材料化学”特色专业立项建设项目、广东第二师范学院教学质量与教学改革工程项目(No.2018zygxk04,2019syzy03)和广东第二师范学院材料化学应用型人才培养课程建设项目(8)资助。
*通信联系人。E-mail:yaosuze@gdei.edu.cn,caomanli@gdei.edu.cn

complex **1-B** in dichloromethane. Crystal structure analysis shows that $[Ru(bpy)_2(DMBbimH)]^+$ cations are bonded by hydrogen bonds to form dimers, which is consistent with the result of the electrochemical measurements. However, hydrogen-bonded dimers couldn't exist stably in the more polar acetonitrile, therefore only one peak existing in the CV curve. CCDC: 2005043, **2**.

Keywords: ruthenium(Ⅱ) polypyridyl complexes; bibenzimidazole; electrochemistry; proton-coupled electron transfer(PCET); crystal structure

Ruthenium (Ⅱ) polypyridyl complexes have been deeply researched because of their excellent redox and photophysical properties, particularly, high stability and absorption and emission spectra in visible range, promising applications as solar energy conversion, molecular electronics, and so on[1-4]. Among them, ruthenium polypyridyl complexes based on biimidazole (H_2biim)[5-10] or bibenzimidazole (H_2bbim)[9-13] or their derivatives moieties[14-19] have received much attention. The presence of the acidic imidazole proton allows deprotonation of the complexes and this results in a rich chemistry where changes in pH can be used to affect the electrochemical and photophysical properties of the complexes[20]. The ability of complexes containing the biimidazole or bibenzimidazole ligands to engage in hydrogen bonding via the externally-directed pair of N-H groups has been exploited extensively in crystal engineering and supramolecular chemistry.

As is well known, hydrogen bonding is one of the most popular tools in supramolecular chemistry because hydrogen bonds have relatively high strength and predictable directional nature compared to other non-covalent interactions[21-23]. There is a growing awareness of the important role that hydrogen-bonded complexes can play in complex electron-transfer mechanisms[24]. The proton-coupled electron transfer (PCET) reactions can occur within hydrogen-bonded intermediates. With incorporation of reversible redox couples and proper designs, electron transfer can provide a convenient means both to detect the hydrogen-bonded complexes and control their assembly.

In this paper, we reported a family of ruthenium(Ⅱ) complexes, namely $[(bpy)_2Ru(DMBbimH_x)]^{y+}$ (DMBbimH_2=7,7′-dimethyl-2,2′-bibenzimidazole, **1-A**: x=2, y=2; **1-B**: x=1, y=1; **1-C**: x=0, y=0). The un-deprotonated **1-A**, mono-deprotonated **1-B** and bi-deprotonated **1-C** were synthesized, and their spectroscopic and electrochemical properties were studied. Interestingly, different electrochemical behaviors of the mono-deprotonated **1-B** were observed in dichloromethane and the more polar acetonitrile. In dichloromethane, it undergoes a two-step oxidation, which indicates the existence of PCET between the $[Ru(bpy)_2(DMBbimH)]^+$ cations.

The single crystals of $[Ru(bpy)_2(DMBbimH)]PF_6\cdot 2CH_2Cl_2$ (**2**), hydrogen-bonded dimer of $[Ru(bpy)_2(DMBbimH)]^+$, were obtained from the solution of **1-B** in dichloromethane. The $[Ru(bpy)_2(DMBbimH)]^+$ cations exist as hydrogen-bonded dimers in dichloromethane, which is consistent with the result of electrochemical measurements of complex **1-B**.

1 Experimental

1.1 Materials and methods

The reagents and solvents employed were commercially available and were used as received. ^{1}H NMR spectra were recorded on a Varian Mercury-Plus 300 NMR spectrometer with chemical shifts relative to tetramethylsilane (TMS). The C, H and N microanalyses were carried out with a Vario EL elemental analyzer. Electron spray ionization (ESI) mass spectra were obtained on an LCQ DECA XP quadrupole ion trap mass spectrometer with methanol as the carrier solvent. UV-Vis spectra were performed on a Shimadzu UV-315 UV-Vis spectrophotometer at room temperature, and the solvents used for spectral experiments were distilled from CaH_2 and kept over molecular sieves (type 4A).

The cyclic voltammetry (CV) and square wave voltammetry (SWV) measurements were made with a CHI-660 Electrochemical Workstation. The experi-

ments were performed with a standard three-electrode arrangement: working electrode, glassy carbon electrode; quasi reference electrode, Ag-AgCl electrode; counter electrode, Pt wire electrode. Background correction was accomplished by subtracting the current curves of the blank electrolyte (containing the same concentration of supporting electrolyte) from the experimental curve. The experiments were performed with 0.001 mol·L^{-1} solutions of the complexes in dried acetonitrile or dried dichloromethane with 0.1 mol·L^{-1} ammonium hexafluorophosphate as supporting electrolyte.

1.2 Syntheses

$DMBbimH_2$[25] and *cis*-$Ru(bpy)_2Cl_2·2H_2O$[26] were synthesized as reported in the literature procedures.

1.2.1 Synthesis of $[Ru(bpy)_2(DMBbimH_2)](PF_6)_2$ (**1-A**)[5]

$[Ru(bpy)_2Cl_2]·2H_2O$ (1 mmol), $DMBbimH_2$ (1.4 mmol) and ethylene glycol (14 mL) were added into a 50 mL three neck flask. The mixture was stirred and refluxed for 3 h under nitrogen protection, then cooled to room temperature and filtered. 100 mL water was added to the filtrate, followed by the addition of 2 mL hydrochloric acid and 0.8 g KPF_6. The mixture was stirred for a while then filtered, and the precipitate was rinsed with water several times then dried at 70 ℃. Yield: 85% on the basis of $[Ru(bpy)_2Cl_2]·2H_2O$. Anal. Calcd. for $C_{36}H_{30}F_{12}N_8P_2Ru$(%): C, 44.78; H, 3.13; N, 11.60. Found(%): C, 45.04; H, 3.32; N, 11.78. ESI-MS (positive, CH_3OH): *m/z* 675.3 ($[Ru(bpy)_2(DMBbimH)]^+$); 338.3 ($[Ru(bpy)_2(DMBbimH_2)]^{2+}$). ^1H NMR (300 MHz, DMSO-d_6): δ 13.84 (s, 2H, N-H), 8.83 (d, *J*=8.2 Hz, 2H, bpy-H), 8.73 (d, *J*=8.1 Hz, 2H, bpy-H), 8.21 (td, *J*=7.8, 1.5 Hz, 2H, bpy-H), 8.04 (td, *J*=7.9, 1.5 Hz, 2H, bpy-H), 7.98 (dd, *J*=5.7, 1.3 Hz, 2H, bpy-H), 7.88 (d, *J*=5.5 Hz, 2H, bpy-H), 7.57 (ddd, *J*=7.2, 5.6, 1.3 Hz, 2H, bpy-H), 7.46 (ddd, *J*=7.0, 5.6, 1.3 Hz, 2H, bpy-H), 7.19 (dd, *J*=7.7, 4.4 Hz, 2H, $DMBbimH_2$-H6), 6.97 (t, *J*=7.7 Hz, 2H, $DMBbimH_2$-H5), 5.45 (d, *J*=8.3 Hz, 2H, $DMBbimH_2$-H4), 2.60 (s, 6H, Me-H).

1.2.2 Synthesis of $[Ru(bpy)_2(DMBbimH)]PF_6$ (**1-B**)

The complex **1-A** was dissolved in the minimum volume of dichloromethane and subjected to column chromatography on neutral alumina (1 cm×10 cm). A red-violet band was eluted with dichloromethane-acetonitrile (3∶1, *V*/*V*). The solvent was evaporated to dryness under vacuum, then the complex **1-B** was obtained with a yield of 75%. Anal. Calcd. for $C_{36}H_{29}F_6N_8PRu$(%): C, 52.75; H, 3.57; N, 13.67. Found (%): C, 52.53; H, 3.63; N, 13.42. ESI-MS (positive, CH_3OH): *m/z* 675.3 ($[Ru(bpy)_2(DMBbimH)]^+$); 338.3 ($[Ru(bpy)_2(DMBbimH_2)]^{2+}$). ^1H NMR (300 MHz, DMSO-d_6): δ 8.77 (d, *J*=8.2 Hz, 2H, bpy-H), 8.68 (d, *J*=8.1 Hz, 2H, bpy-H), 8.14 (td, *J*=7.9, 1.4 Hz, 2H, bpy-H), 8.06~7.88 (m, 4H, bpy-H), 7.76 (d, *J*=5.6 Hz, 2H, bpy-H), 7.52 (ddd, *J*=7.2, 5.6, 1.2 Hz, 2H, bpy-H), 7.44 (ddd, *J*=7.1, 5.5, 1.3 Hz, 2H, bpy-H), 6.85 (d, *J*=7.2 Hz, 2H, DMBbimH-H6), 6.66 (t, *J*=7.7 Hz, 2H, DMBbimH-H5), 5.31 (d, *J*=8.1 Hz, 2H, DMBbimH-H4), 2.55 (s, 6H, Me-H).

1.2.3 Synthesis of $Ru(bpy)_2(DMBbim)$ (**1-C**)

The complex **1-A** was dissolved in a small amount of methanol, and an excessive amount of ammonia gas was introduced[27], and the precipitate was filtered to obtain the complex **1-C**. Yield: 50%. Anal. Calcd. for $C_{36}H_{28}N_8Ru$(%): C, 64.18; H, 4.19; N, 16.63. Found (%): C, 62.37; H, 4.02; N, 16.36. ESI-MS (positive, CH_3OH): *m/z* 675.3 ($[Ru(bpy)_2(DMBbimH)]^+$); 338.3 ($[Ru(bpy)_2(DMBbimH_2)]^{2+}$). ^1H NMR (300 MHz, DMSO-d_6): δ 8.69 (d, *J*=8.2 Hz, 2H, bpy-H), 8.60 (d, *J*=8.1 Hz, 2H, bpy-H), 8.04 (t, *J*=7.8 Hz, 2H, bpy-H), 7.89 (d, *J*=5.5 Hz, 2H, bpy-H), 7.83 (t, *J*=7.8 Hz, 2H, bpy-H), 7.73 (d, *J*=5.5 Hz, 2H, bpy-H), 7.45 (t, *J*=6.6 Hz, 2H, bpy-H), 7.36 (t, *J*=6.6 Hz, 2H, bpy-H), 6.52 (d, *J*=7.0 Hz, 2H, DMBbim-H6), 6.32 (t, *J*=7.5 Hz, 2H, DMBbim-H5), 5.16 (d, *J*=7.9 Hz, 2H, DMBbim-H4), 2.49 (s, 6H, Me-H).

1.2.4 Synthesis of $[Ru(bpy)_2(DMBbimH)]PF_6·2CH_2Cl_2$ (**2**)

Single crystals of **2** were grown at room temperature by slow evaporation of the solution of **1-B** in dichloromethane. Dark red single crystals were obtained about one week later. Anal. Calcd. for $C_{38}H_{33}Cl_4F_6N_8PRu$(%): C, 46.12; H, 3.36; N, 11.32. Found(%): C, 46.05; H, 3.43; N, 11.27.

1.3 Structure determination

The intensity data for compound **2** were collected

on a Bruker Smart Apex CCD area detector, using graphite-monochromated Mo $K\alpha$ radiation (λ=0.071 073 nm). The structure was solved by direct method and refined by full matrix least squares techniques against F^2 (SHELXTL-2016 program package[28-29]). The hydrogen atoms of the "amine group" were located by Fourier difference synthesis and refined isotropically. All other hydrogen atoms were included at calculated positions with fixed thermal parameters. All non-hydrogen atoms were refined anisotropically. The solvents were squeezed by SQUEEZE/PLATON program. Crystal data, data collection parameters and refinement statistics are listed in Table 1. Selected bond lengths and angles are presented in Table 2.

CCDC: 2005043, **2**.

Table 1 Crystal data and structure parameters for complex 2

Empirical formula	$C_{38}H_{33}Cl_4F_6N_8PRu$	F(000)	3 984
Formula weight	989.56	Crystal size / mm	0.230×0.200×0.160
Crystal system	Monoclinic	θ range for data collection / (°)	3.094~25.999
Space group	$C2/c$	Limiting indices	$-39 \leqslant h \leqslant 39$, $-20 \leqslant k \leqslant 20$, $-21 \leqslant l \leqslant 23$
a / nm	3.182 7(2)	Reflection collected, unique	36 729, 8 972 (R_{int}=0.108 5)
b / nm	1.638 4(1)	Reflection observed	6 835
c / nm	1.885 3(1)	Completeness to θ=25.242 / %	99.7
β / (°)	111.255(2)	Data, restraint, parameter	8 972, 0, 469
V / nm^3	9.162(1)	Goodness-of-fit on F^2	1.032
Z	8	Final R indices [$I>2\sigma(I)$]	R_1[a]=0.067 8, wR_2[b]=0.175 6
D_c / (g·cm^{-3})	1.435	R indices (all data)	R_1[a]=0.086 6, wR_2[b]=0.189 1
Absorption coefficient / mm^{-1}	0.671		

[a] $R_1=\sum||F_o|-|F_c||/\sum|F_o|$; [b] $wR_2=[\sum w(F_o^2-F_c^2)^2/\sum w(F_o^2)^2]^{1/2}$.

Table 2 Selected bond lengths (nm) and angles (°) for complex 2

Ru1-N1	0.204 3(4)	Ru1-N2	0.204 7(4)	Ru1-N3	0.205 4(4)
Ru1-N4	0.205 2(4)	Ru1-N5	0.208 9(4)	Ru1-N7	0.210 8(4)
C21-N5	0.138 9(6)	C28-N5	0.133 6(6)	C26-N6	0.138 8(6)
C28-N6	0.135 4(6)	C29-N7	0.134 7(6)	C30-N7	0.138 9(6)
C29-N8	0.134 8(6)	C35-N8	0.139 9(6)	C28-C29	0.144 4(6)
N2-Ru1-N1	78.6(2)	N4-Ru1-N3	78.8(2)	N5-Ru1-N7	78.3(1)
N2-Ru1-N3	89.0(2)	N4-Ru1-N5	85.1(1)	N1-Ru1-N7	85.8(1)
N3-Ru1-N5	95.6(1)	N2-Ru1-N7	97.6(2)	N1-Ru1-N5	95.4(1)
N4-Ru1-N7	94.9(2)	N3-Ru1-N1	100.5(2)	N2-Ru1-N4	100.9(2)
N4-Ru1-N1	179.2(1)	N2-Ru1-N5	173.0(1)	N3-Ru1-N7	171.7(1)
C31-C30-C35	120.3(4)	C22-C21-C26	121.0(4)	C24-C25-C26	115.4(4)
N7-C30-C35	108.3(4)	C23-C22-C21	116.5(4)	C24-C25-C27	124.0(5)
C30-C31-C32	117.1(4)	C22-C23-C24	122.0(5)	C26-C25-C27	120.6(4)
N5-C21-C22	131.3(4)	C25-C24-C23	122.9(5)	N6-C26-C25	129.5(4)
N5-C21-C26	107.7(4)	C1-N1-C5	117.5(4)	N6-C26-C21	108.2(4)
C25-C26-C21	122.2(4)	C10-N2-C6	118.0(4)	N7-C29-C28	116.1(4)
N5-C28-N6	115.3(4)	C11-N3-C15	118.9(4)	N8-C29-C28	129.1(4)
N5-C28-C29	117.3(4)	C20-N4-C16	118.5(4)	C31-C30-N7	131.4(4)
N6-C28-C29	127.4(4)	N7-C29-N8	114.9(4)	C31-C32-C33	122.2(5)
C28-N5-C21	104.7(4)	C29-N8-C35	104.8(4)	C34-C33-C32	122.3(5)

Continued Table 2

C28-N6-C26	104.0(4)	C33-C34-C35	115.7(4)	C33-C34-C36	122.3(4)
C29-N7-C30	104.7(4)	C35-C34-C36	122.0(4)	C34-C35-N8	130.2(4)
C34-C35-C30	122.4(4)	N8-C35-C30	107.4(4)		

2 Results and discussion

2.1 Synthesis

Reaction between *cis*-$Ru(bpy)_2Cl_2 \cdot 2H_2O$ and $DMBbimH_2$ in refluxing ethylene glycol resulted in the formation of $Ru(bpy)_2(DMBbimH_2)](PF_6)_2$, **1-A**, which can be converted into mono-deprotonated **1-B** and bi-deprotonated **1-C** under suitable condition. The reactions in Fig. 1 are reversible and each of the three species involved can be converted into any one of the other two simply by the adjustment of pH. We have been able to isolate all of the three species in their pure states.

The mass spectra of these complexes were nearly identical, where peaks at 675.3 and 338.3 can be assigned to $[Ru(bpy)_2(DMBbimH)]^+$ and $[Ru(bpy)_2(DMBbimH_2)]^{2+}$. This helps us to confirm the structures of the complexes to some extent. However, the ^1H NMR (section 2.2), UV-Vis spectra (section 2.3), and electrochemical properties (section 2.4) of the complexes **1-A**, **1-B**, and **1-C** showed obvious differences. Single crystals were grown from the dichloromethane solution of **1-B**. The molecular structure of compound $[Ru(bpy)_2(DMBbimH)]PF_6 \cdot 2CH_2Cl_2$ (2) has been confirmed by X-ray crystallography (section 2.5).

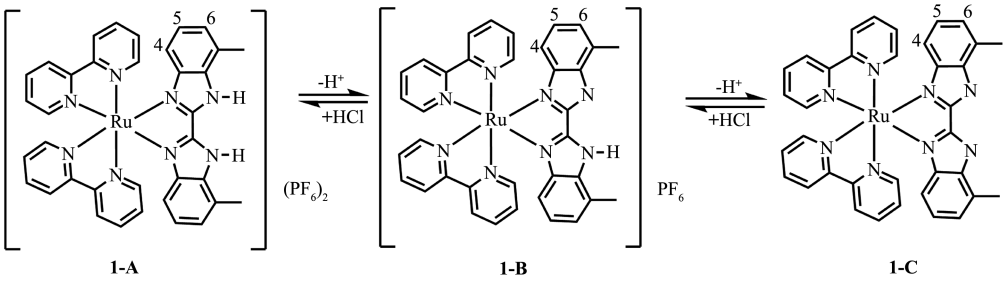

Fig.1　Structures and reactions of complexes **1-A**, **1-B** and **1-C**

2.2 ^1H NMR

NMR spectroscopy has proved to be a useful tool in the structural characterization of ruthenium polypyridyl complexes[30]. We confirm the structures of complexes **1-A**, **1-B** and **1-C** through their ^1H NMR spectra (Fig. 2) which were recorded in DMSO-d_6 at room temperature.

In the spectrum of **1-A**, the four doublets and four triplets between δ 8.83 and δ 7.46 belong to the aromatic protons of bpy groups. The relative intensities of these resonances were, as expected, 1∶1∶1∶1∶1∶1∶1∶1. The doublet at δ 7.19, triplet at δ 6.97, doublet at δ 5.45 can be respectively assigned to the aromatic protons H6, H5 and H4 of $DMBbimH_2$, and a singlet at δ 2.60 can be assigned to the methyl group of $DMBbimH_2$. In the spectrum of **1-A**, there was a broad signal at δ 13.80. The broadness and extreme low-field shift suggest that it corresponds to the N-H protons of $DMBbimH_2$.

In the spectrum of **1-B**, two of resonances of the bpy group were overlapped at δ 8.06~7.88. With the removal of the first proton, the signal of N-H proton disappeared, signals of H4, H5 and H6 of complex **1-B** shifted towards the up-field region by 0.14, 0.31 and 0.34, respectively. The chemical shift of the methyl group protons is at δ 2.55.

For **1-C**, the varieties of chemical shifts of bpy group and methyl group (δ 2.49) protons were smaller, while the aromatic protons of DMBbim ligand exhibited a larger shift. With the removal of the second proton, signals of H4, H5 and H6 of complex **1-C** further shifted towards the up-field region by 0.15, 0.34 and 0.33, respectively. This is because that as the bibenzimidazole ligand is gradually deprotonated, the overall electron cloud density of the ligand increases.

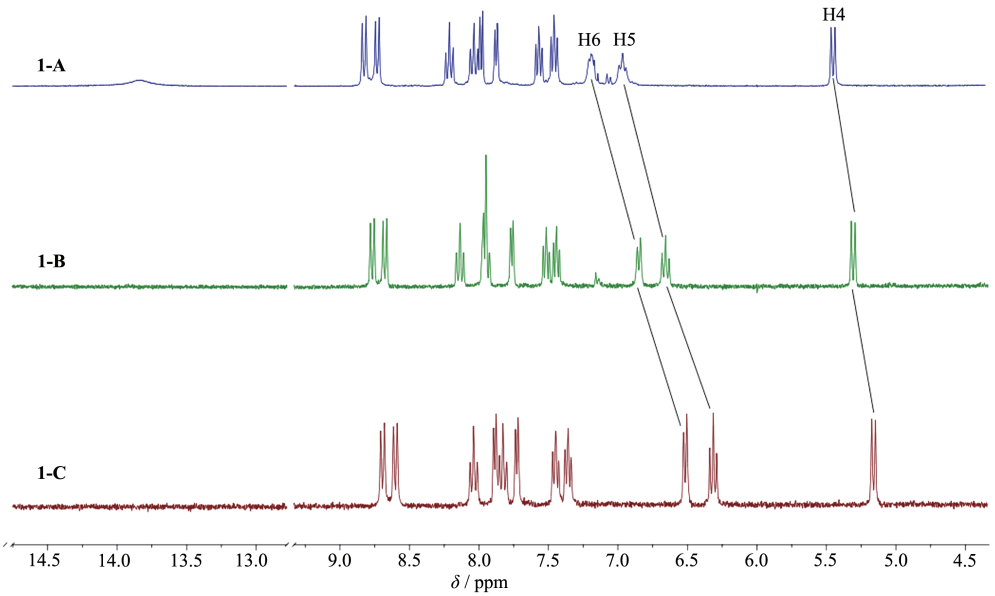

Fig.2 ^{1}H NMR spectra of complexes **1-A**, **1-B** and **1-C** in DMSO-d_6

H4, H5 and H6 are getting closer and closer to the dehydrogenated N atoms, so they are gradually affected by dehydrogenation.

2.3 Absorption spectral studies.

Absorption spectral profiles of the complexes in acetonitrile are presented in Fig.3, and the related data are summarized in Table 3. In order to compare the relative intensity of the absorption bands, iso-molar solutions (60 μmol·L^{-1}) of the complexes were used.

The highly intense absorption bands observed in UV region arise mainly due to the π-π* transitions within the bpy and DMBbimH$_x$ units[15,31]. The strong absorption band at 290~300 nm can be attributed to π-π* transition of bpy ligand. The 335 nm absorption band of **1-A**, 341 nm band of **1-B**, 338 nm band of **1-C**, are assigned to π-π* transition of the DMBbimH$_x$ ligands, respectively. The moderately intense broad bands in visible region can be attributed to M($d\pi$)→bpy(π*) and M($d\pi$)→DMBbimH$_x$(π*) MLCT transitions.

In the absorption spectral profiles, it was observed

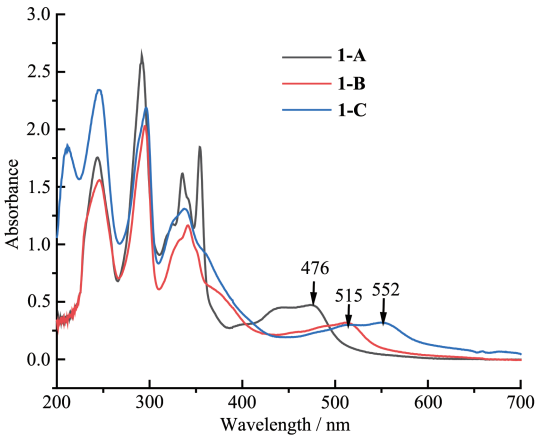

Fig.3 UV-Vis absorption spectra of iso-molar acetonitrile solutions of complexes **1-A**, **1-B** and **1-C**

that the MLCT bands in the complexes underwent gradual red-shifts. With the removal of protons, the absorption peak was red-shifted from 476 nm (**1-A**) to 515 nm (**1-B**) and finally to 552 nm (**1-C**). This is because the interaction (mono-deprotonation or bi-deprotonation in DMBbimH$_x$ ligand) greatly increases the electron density at the Ru(Ⅱ) center and leads to a less-positive oxida-

Table 3 Absorption spectroscopic data for complexes in acetonitrile

Complex	λ_{max} / nm
1-A	244(sharp), 292(sharp), 335(sharp), 354(sharp), 476(broad)
1-B	246(sharp), 295(sharp), 341(moderate), 515(broad)
1-C	212(sharp), 247(sharp), 296(sharp), 338(moderate), 552(broad)

tion potential (section 2.4), resulting in the decrease of MLCT band energy.

2.4 Electrochemistry

Electrochemical behaviors of the complexes in dichloromethane and acetonitrile were studied through CV and SWV methods using Ag/AgCl reference electrode and ammonium hexafluorophosphate as supporting electrolyte. $E_{1/2}$ values were obtained from SWV using glassy carbon electrode.

As shown in Fig.4, in dichloromethane, the mononuclear complex **1-A** underwent oxidation irreversibly at 1.35 V. CV and SWV measurements of **1-B** in dichloromethane revealed characteristic phenomena for cooperative proton electron transfer. Two successive electrode oxidation couples ($E_{1/2,1}$=0.97 V and $E_{1/2,2}$= 1.33 V (vs Ag/AgCl)) were observed, revealing that the complex undergoes two successive one-electron reversible oxidation processes due to Ru(Ⅱ)-Ru(Ⅱ)/Ru(Ⅲ)-Ru(Ⅱ) and Ru(Ⅲ)-Ru(Ⅱ)/Ru(Ⅲ)-Ru(Ⅲ) processes, respectively. This is due to the presence of hydrogen-bonded dimers in **1-B**. In **1-B**, there is only one N-H bond on the DMBbimH ligand. Two $[Ru(bpy)_2(DMBbimH)]^+$ cations are easily bonded by hydrogen bonds to form a dimer structure, which can not only exist in solid state, but also exist stably in weak polar solvents. The redox of two Ru centers in the dimer is not completely symmetrical and simultaneous. One of the metal centers Ru(Ⅱ) is oxidized to Ru(Ⅲ) first (Fig.5), and then the other metal center is oxidized. The extent of electronic interaction between two metal centers in homo-bimetallic complexes can be estimated from the differences between two oxidation potentials ($\Delta E_{1/2}=|E_{1/2,2}-E_{1/2,1}|$)[15]. $\Delta E_{1/2}$ value obtained in this way was 0.36 V.

The doubly deprotonated complex **1-C** underwent oxidation irreversibly at 0.71 V in dichloromethane. As expected, deprotonation of the bi-benzimidazole ligand leads to shifts towards more negative potentials for the oxidation of the ruthenium center. This indicates an enhanced electron density at the metal center induced by deprotonation[11].

As we know, the polarity of solvent has a great effect on the formation of hydrogen-bonded species and the electrochemical properties of complexes. Therefore, the electrochemical behaviors of the complexes in acetonitrile, whose polarity is much stronger than dichloromethane, were explored. The CV and SWV of the

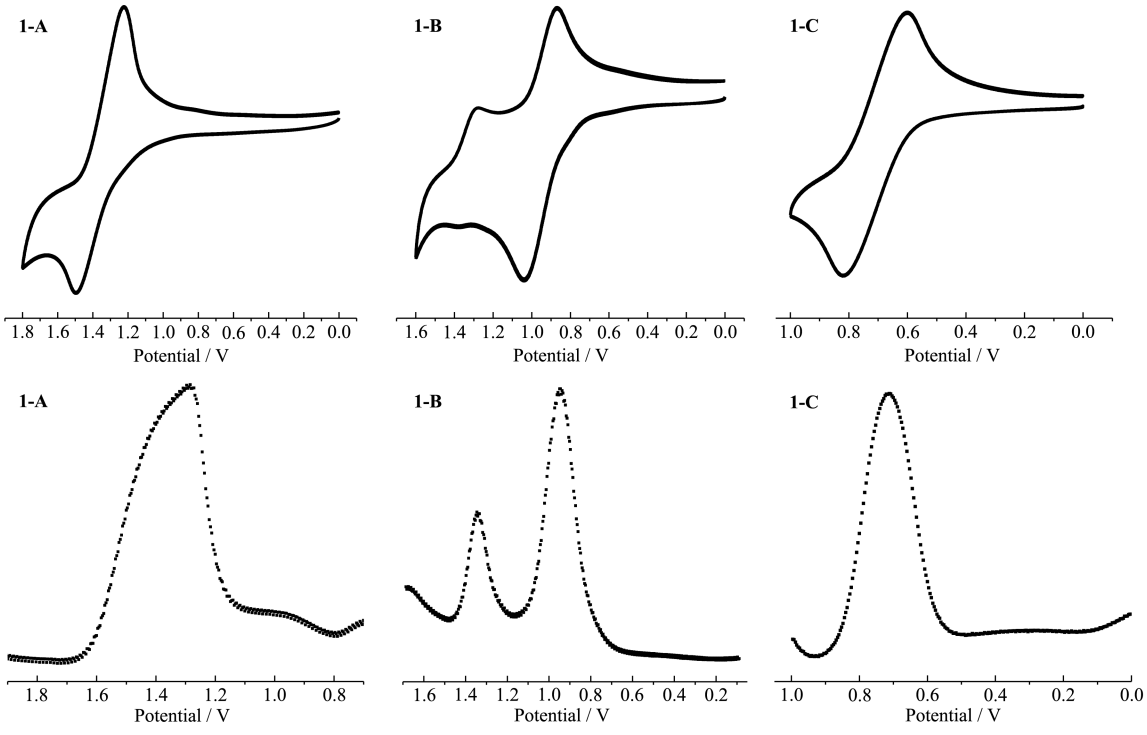

Fig.4　CV and SWV of **1-A**, **1-B**, **1-C** in dichloromethane

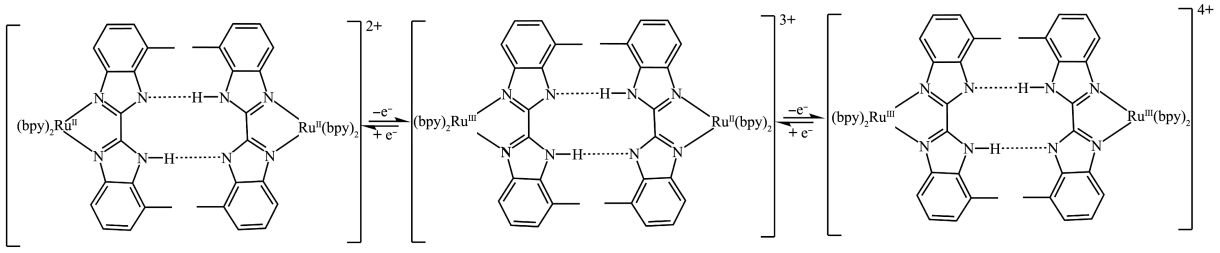

Fig.5 Redox reactions of hydrogen bonding dimer in **1-B**

complexes are shown in Fig. 6. In the curves we can easily find that each complex exhibited a reversible wave corresponding to Ru(Ⅱ)/Ru(Ⅲ) oxidation process in acetonitrile. Ru(Ⅱ)/Ru(Ⅲ) oxidation potential gradually shifted towards lower potential as the complex was changed from **1-A** ($E_{1/2}$=1.22 V) to **1-B** ($E_{1/2}$=0.88) and finally to **1-C** ($E_{1/2}$=0.57 V) and this is line with the observed absorption spectral trends.

Comparing Fig.4 and Fig.6, we can easily find out that the electrochemical properties of complex **1-B** in dichloromethane and acetonitrile differ greatly, which is due to the different polarities of solvents. In dichloromethane, mononuclear complex **1-B** undergoes a two-step oxidation, which indicates the existence of PCET between $[Ru(bpy)_2(DMBbimH)]^+$ cations. The $[Ru(bpy)_2(DMBbimH)]^+$ cations exist as hydrogen-bonded dimers in dichloromethane, and the existence of hydrogen-bonded dimers is proved by single crystal structure (section 2.5). However, the dimers cannot exist stably in more polar acetonitrile, and the cations exist as monomers, therefore, only one peak can be observed on CV and SWV curves.

In conclusion, for **1-B**, dimers are formed preferentially over the corresponding monomers in weakly polar solvents, such as dichloromethane. CV measurements show that **1-B** reversibly generates stable mixed-valence states $Ru^{Ⅱ}Ru^{Ⅲ}$ upon oxidation. As a result, it is reasonable that the mixed-valence states are stabilized by proton transfer of complementary hydrogen bonds[27].

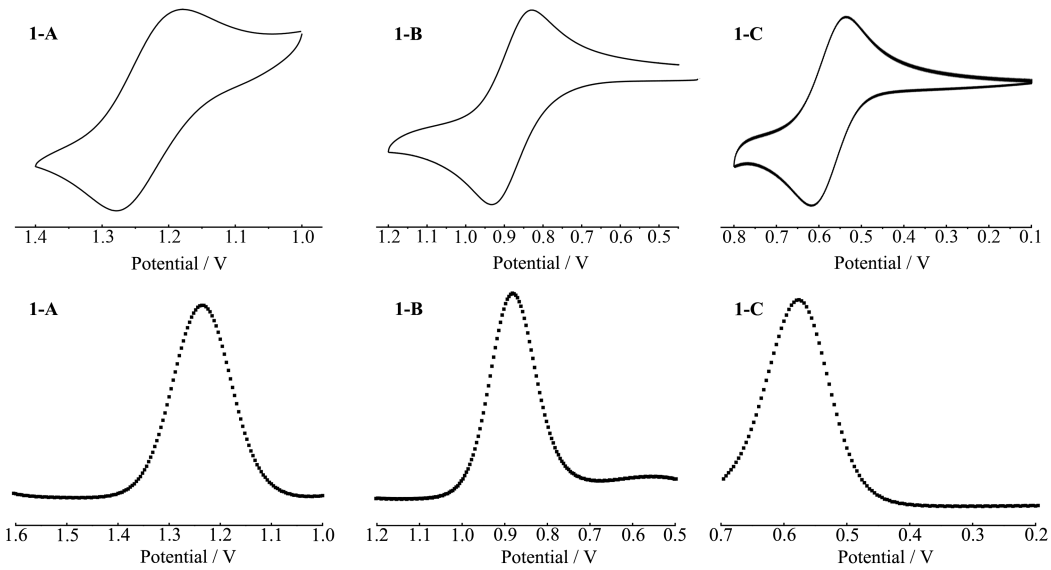

Fig.6 CV and SWV of **1-A**, **1-B** and **1-C** in acetonitrile

2.5 Single-crystal structure of 2

Dark red single crystals of complex $[Ru(bpy)_2(DMBbimH)]PF_6\cdot 2CH_2Cl_2$ (**2**) were obtained from dichloromethane solution of **1-B**. The single crystal structure of **1-B** indicates that it belongs to *C*2/*c* space group of monoclinic system. Each asymmetric unit contains a $[Ru(bpy)_2(DMBbimH)]^+$ cation, a PF_6^- anion and two dichloromethane molecules. The components are

supported by elemental analysis data. The solvents were squeezed by SQUEEZE/PLATON program because the dichloromethane molecules were disordered.

As shown in Fig.7a, each Ru(Ⅱ) ion is coordinated with six N atoms from two bpy ligands and one DMBbimH$^-$ ligand to form an octahedral coordination geometry. The Ru-N bond length between Ru(Ⅱ) ion and bpy is between 0.204 3(4) and 0.205 4(4) nm, and the Ru-N bond length with DMBbimH$^-$ ligand is slightly longer (0.208 9(4)~0.210 8(4) nm), but agrees with literature values[5-19]. The N-Ru-N bite angles vary from 78.3° to 78.8°, while the *trans* angles lie in a range of 171.7(2)° ~179.2(2)°. The DMBbimH$^-$ ligand coordinates in a bidentated manner with N5 and N7, remaining the other two N atoms (N6 and N8) uncoordinated. The hydrogen atoms on N6 and N8 are disordered, and H6A and H8A are both half-occupied due to the symmetry. Each $[Ru(bpy)_2(DMBbimH)]^+$ cation pairs up with a symmetry-equivalent cation to generate a dimeric unit $[Ru(bpy)_2(DMBbimH]_2^{2+}$ containing a self-complementary double hydrogen-bonded bridge (Fig. 7a). The N6···N6A separation is 0.271 5 nm and the N6-H6A-N6A angle is 166.5°, and the N8···N8A separation is 0.278 5 nm and the N8-H8A-N8A angle is 172.9°. Only half of hydrogen atoms (H6A and H8A) are presented in Fig.7a. The Ru···Ru distance defined by this supramolecular arrangement is 1.011 9 nm.

The dihedral angle between the planes of two benzimidazole in a DMBbimH$^-$ ligand is 6.2°, indicating an almost planar structure of the DMBbimH$^-$ moiety in **2**. It is worth mentioning that the angle between two DMBbimH$^-$ ligands in a dimer is twisted to about 57.2° (Fig.7b), which should be attributed to the side-by-side steric repulsion between the methyl groups at the 7 and 7′ positions.

There are abundant weak intermolecular forces in the structure, as shown in Fig. 8[32]. The cations and anions are connected by C–H···F weak hydrogen bonds (Table 4) to form two-dimensional layers, which

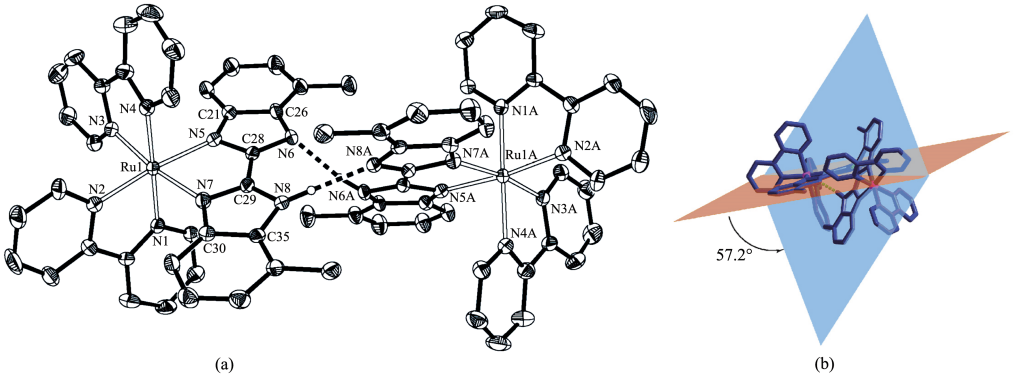

Dashed lines indicate hydrogen bonds; Anions, solvent molecules and hydrogen atoms, except for N6 and N8 are omitted for clarity; Symmetry code: A: $-x+1, y, -z+3/2$

Fig.7　Structure as an ORTEP drawing with 30% probability thermal ellipsoids (a) and dihedral angle (b) of hydrogen-bonded dimer in **2**

Table 4　Selected hydrogen bond parameters in 2

D–H···A	*d*(D-H) / nm	*d*(H···A) / nm	*d*(D···A) / nm	∠DHA / (°)
C11–H11···F5	0.093	0.254	0.342 0(8)	157.7
C12–H12···F1	0.093	0.258	0.325 0(9)	128.9
C14–H14···F2A	0.093	0.242	0.328 8(7)	155.6
C19–H19···F3B	0.093	0.262	0.354 8(9)	172.0
C19–H19···F5B	0.093	0.252	0.326 2(7)	136.8
N6–H6···N6C	0.088	0.186	0.272 1(8)	166.6
N8–H8···N8C	0.089	0.191	0.280 0(7)	172.9

Symmetry codes: A: $-x+1/2, -y+3/2, -z+1$; B: $x, -y+1, z+1/2$; C: $-x+1, y, -z+3/2$.

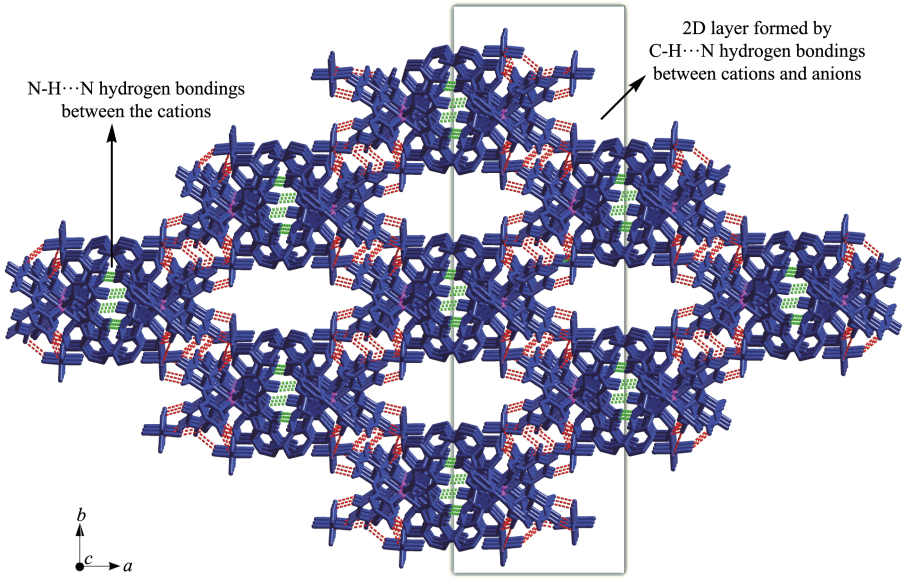

Green lines, N−H···N hydrogen bonds; Red lines, C−H···F hydrogen bonds

Fig.8 Three-dimensional network formed by hydrogen bonds in **2**

are linked into three-dimensional network by N−H···N hydrogen bonds between cations. The solvent molecules fill in one-dimensional channels along the *c*-axis direction formed by the cations and anions.

3 Conclusions

In summary, three ruthenium(Ⅱ) polypyridyl complexes containing 7,7′-dimethyl-2,2′-bibenzimidazole ligand ($DMBbimH_x$) were synthesized and determined by ^1H NMR, UV-Vis absorption and electrochemical measurements. From **1-A** to **1-B** and then to **1-C**, N-H in $DMBbimH_x$ ligands gradually deprotonated, resulting in evident differences of the spectroscopic and electrochemical properties of complexes. Interestingly, for mono-deprotonated **1-B**, the electrochemical properties behaved very differently in dichloromethane and acetonitrile, which is due to different polarities of solvents. In acetonitrile, there was only one redox peak in CV curve, while in dichloromethane, it underwent a two-step oxidation, which indicates the existence of PCET in hydrogen-bonded dimers formed by $[Ru(bpy)_2(DMBbimH)]^+$ cations. The single crystal structure of **2** indicates that $[Ru(bpy)_2(DMBbimH)]^+$ cations exist as hydrogen-bonded dimers in weakly polar solvent dichloromethane. This is consistent with the result of electrochemical measurements of complex **1-B** in dichloromethane.

References:

[1] D′Alessandro D M, Keene F R. *Chem. Rev.*, **2006**, **106**(6): 2270-2298

[2] Kaim W, Lahiri G K. *Angew. Chem., Int. Ed.*, **2007**,**46**:1778-1796

[3] D′Alessandro D M, Keene F R. *Chem. Soc. Rev.*, **2006**,**35**:424-440

[4] Gill M R, Thomas J A. *Chem. Soc. Rev.*, **2012**,**41**:3179-3192

[5] Dose E V, Wilson L J. *Inorg. Chem.*, **1978**,**17**:2660-2666

[6] Majumdar P, Peng S M, Goswami S. *J. Chem. Soc. Dalton Trans.*, **1998**:1569-1574

[7] Cui Y, Mo H J, Chen J C, et al. *Inorg. Chem.*, **2007**,**46**:6427-6436

[8] Derossi S, Adams H, Ward M D. *Dalton Trans.*, **2007**:33-36

[9] Mo H J, Niu Y L, Zhang M, et al. *Dalton Trans.*, **2011**, **40**: 8218-8225

[10]Mo H J, Wu J J, Qiao Z P, et al. *Dalton Trans.*, **2012**,**41**:7026-7036

[11]Rau S, Ruben M, Buttner T, et al. *J. Chem. Soc. Dalton Trans.*, **2000**:3649-3657

[12]Cui Y, Niu Y L, Cao M L, et al. *Inorg. Chem.*, **2008**,**47**:5616-5624

[13]Xu H B, Chen X L, Deng J G, et al. *Dalton Trans.*, **2018**,**47**: 2073-2078

[14]Mardanya S, Karmakar S, Bar M, et al. *Dalton Trans.*, **2015**, **44**:21053-21072

[15]Mardanya S, Karmakar S, Mondal D, et al. *Inorg. Chem.*, **2016**,**55**(7):3475-3489

[16]Mondal D, Baitalik S. *ChemistrySelect*, **2016**,**1**:1318-1328

[17]Mo H J, Chao H Y, Ye B H. *Inorg. Chem. Commun.*, **2013**, **35**:100-103

[18]Yin J, Elsenbaumer R L. *Inorg. Chem.*, **2007**,**46**:6891-6901

[19]Heussner K, Peutinger K, Rockstroh N, et al. *Dalton Trans.*, **2015**,**44**:330-337

[20]Haga M, Tsunemitsu A. *Inorg. Chim. Acta*, **1989**,**164**:137-142

[21]Braga D, Grepioni F, Desiraju G R. *Chem. Rev.*, **1998**, **98**: 1375-1406

[22]Braga D, Maini L, Polito M, et al. *Coord. Chem. Rev.*, **2003**, **246**:53-71

[23]Brammer L. *Chem. Soc. Rev.*, **2004**,**33**:476-489

[24]Clare L A, Pham A T, Magdaleno F, et al. *J. Am. Chem. Soc.*, **2013**,**135**:18930-18941

[25]Muller E, Bernardinelli G, Reedijk J. *Inorg. Chem.*, **1995**,**34**: 5979-5988

[26]Sprintschnik G, Sprintschnik H W, Kirsch P P, et al. *J. Am. Chem. Soc.*, **1977**,**99**:4947-4954

[27]Tadokoro M, Inoue T, Tamaki S, et al. *Angew. Chem. Int. Ed.*, **2007**,**46**(31):5938-5942

[28]Sheldrick G M. *Acta Crystallogr. Sect. A*, **2015**,**A71**:3-8

[29]Sheldrick G M. *Acta Crystallogr. Sect. C*, **2015**,**C71**:3-8

[30]Lees A C, Evrard B, Keyes T E, et al. *Eur. J. Inorg. Chem.*, **1999**,**12**:2309-2317

[31]Juris A, Balzani V. *Coord. Chem. Rev.*, **1988**,**84**:85-277

[32]Zhang X D, Hua J A, Guo J H, et al. *J. Mater. Chem. C*, **2018**,**6**:12623-12630